JOURNAL OF MATERIALS SCIENCE 21 (1986) 3065–3070

Precipitation behaviour of a sensitized AISI type 316 austenitic stainless steel in hydrogen

P. ROZENAK, D. ELIEZER
Department of Materials Engineering, Ben Gurion University of the Negev, Beer Sheva, Israel

The purpose of this study was to characterize the precipitation behaviour of AISI type 316 steel in hydrogen. The different precipitates ($M_{23}C_6$, M_6C), the intermetallic χ-phase and the martensitic phase (α', ε) were determined by using transmission electron microscopy (TEM) and X-ray diffraction techniques. All the specimens were sensitized at 650° C for 24 h. Some samples were carburized up to 2 wt% C. Additions of carbon content decrease the time required for sensitization. Short-term (24 h) exposure of this steel to sensitization temperature results in a complex precipitation reaction of various carbides and intermetallic phases. Hydrogen was introduced by severe cathodic charging at room temperature. This study indicates that by conventional X-ray techniques it is possible to detect those precipitates and their behaviour in a hydrogen environment. The zero shift as observed by X-ray diffraction from the carbides ($M_{23}C_6$, M_6C) and the intermetallic χ-phase, indicates that those phases absorb far less hydrogen than the austenitic matrix. TEM studies reveal that hydrogen induces α' martensite at chromium-depleted grain-boundary zones, near the formation of the carbides.

1. Introduction

AISI type 316 stainless steel is widely used in the power generating industry and is also extensively used as an economical structural material and cladding alloy in conventional and advanced nuclear reactors. Long-term exposure of type 316 to elevated temperature is known to cause decomposition of the austenitic matrix resulting in the formation of several carbides and intermetallic phases. However, literature data on the microstructural changes occurring during long-term service exposure in a hydrogen environment are very scarce. Carbon is present in all austenitic steels and plays a major role in the sensitization process [1, 2].

Owing to the complexity of the precipitation process, phase identification in type 316 is difficult [2–4]. By conventional X-ray techniques it is difficult to draw the line between detected or not detected when small amounts of carbides and intermetallic phases are involved. To overcome these difficulties we carburized our specimens by using a carbon-coating method. This process raised the carbon content, which increased the amount and the size of the precipitates in the steel.

The purpose of the present study was to characterize the precipitates and phase transformations that occur in the presence of a hydrogen environment and the effect of hydrogen solubility on the different carbides.

2. Experimental procedure

The studies were carried out on AISI type 316 austenitic stainless steel. The steel was of commercial grade, of composition shown in Table I, and was received in the form of sheets 0.1 mm thick. All of the samples used in these experiments were solution annealed for 1 h at 1100° C and then water quenched. The grain size as measured by ASTM E-112 method [5], was ASTM 11. Some samples were carburized by using carbon coating at 1100° C for 6 h. The carbon concentration in this specimen is about 2 wt %. All the specimens were sensitized at 650° C for 24 h. Hydrogen charging was performed at room temperature in 1 N H_2SO_4 solution with 0.25 g l^{-1} $NaAsO_2$ added as a hydrogen recombination poison. A platinum counter electrode and a current density of 50 mA cm^{-2} were used. A conventional Philips diffractometer equipped with step-motor and Co$K\alpha$ radiation was used for X-ray diffraction study. The microstructures of the various carbides, martensitic and second phases were determined by using transmission electron microscopy (TEM). TEM analysis was carried out in a JEOL-200B electron microscope operating at 150 kV. Specimens suitable for electron microscopy were prepared by electrolytic polishing at 65 V in a Tenupol polishing cell using 30 cm^3 perchloric acid, 300 cm^3 methanol and 520 cm^3 butanol solution at −18° C. The morphology of the different carbides and surface cracking were examined using a scanning electron microscope (SEM).

3. Results and discussion

X-ray diffraction results, obtained from the various treatments of AISI type 316 steel before and after

TABLE I Chemical composition of type 316 austenitic stainless steel (elements wt %)

Cr	Ni	Mn	Si	C	Mo
16.8	13.2	1.70	0.41	0.03	2.08

0022–2461/86 $03.00 + .12

TABLE II *d*-spacing of sensitized AISI type 316 stainless steel, as-received, carburized and cathodically charged

Phases, crystal structure						This investigation				Reported in literature					
χ bcc	M_6C fcc	$M_{23}C_6$ fcc	ε hcp	α' bcc	γ fcc	As-received (nm)	Carburized (nm)	Cathodically* charged (nm)	Carburized* and cathodically charged (nm)	χ [6] (nm)	M_6C [7] (nm)	$M_{23}C_6$ (nm)	ε (nm)	α-Fe (nm)	γ-Fe [8] (nm)
		420					0.2368		0.2373			0.236			
	422						0.2292		0.2294		0.229				
400							0.2215		0.2215	0.222					
	333	422					0.2162		0.2167		0.216	0.215			
330							0.2105		0.2105	0.209					
					111	0.2075	0.2082	0.2082	0.2071						0.208
		333					0.2044		0.2038			0.203			
				110				0.2030	overlap					0.2026	
			01.1					0.1964	0.1954				0.1942		
	440							0.2019			0.198				
332	531						0.1890		0.1884	0.189	0.189				
	442						0.1875				0.187				
		440					0.1837		0.1844	0.1865					
442		531					0.1803		0.1808	0.181		0.180			
					200	0.1800	0.1822	0.1800							0.180
431							0.1750		0.1748	0.174					
622	733						0.1346			0.134	0.135				
					220	0.1271	0.1271	0.1271	0.1269						0.127
550							0.1254		0.1251	0.126					
522							0.1205		0.1204	0.121					
	755						0.1181		0.1183		0.1126				
730							0.1167		0.1168	0.117					
					311	0.1083	0.1083	0.1083	0.1083						0.1083
					222	0.1036	0.1037	0.1036	0.1036						0.1037

*XRD analysis was performed after ageing for 24 h.

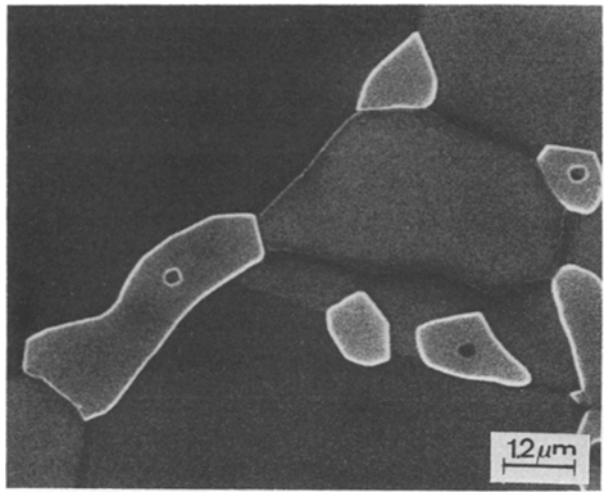

Figure 1 Scanning electron micrographs of the morphology and distribution of the different carbides in AISI type 316 sensitized and carburized steel.

TABLE III Crystal structure of phases in sensitized AISI type 316 stainless steel

Phase	Crystal structure	Lattice parameters		
		This investigation (nm)	Literature (nm)	
$M_{23}C_6$	fcc	1.055	1.0680	[12]
			1.0638	[13]
			1.055	[7]
M_6C	fcc	1.120	1.120	[7]
			1.185	[14]
Chi (χ)	bcc α-Mn structure	0.889	0.8920	[15]
			0.8862	[12]
			0.889	[6]

hydrogen charging are summarized in Table II. The diffraction patterns of sensitized steel reveals the presence of $M_{23}C_6$, M_6C carbides and intermetallic phase χ that are formed after the carburizing treatment. Scanning electron micrographs of various phases that appear in carburized specimens after sensitization are shown in Fig. 1. The different particles (Fig. 1) were identified by TEM. Examination of the microstructures revealed $M_{23}C_6$ carbides (Fig. 2). The sizes of the particles were in the range 2.5 to 100 nm. Diffraction patterns and their schematic key diagram (Figs. 2b, c) from the $M_{23}C_6$ carbide shows fcc crystal structure with a lattice parameter of 1.055 nm. The $M_{23}C_6$, M_6C carbides and intermetallic χ-phase appeared after 24 h sensitization (at 650° C). In uncarburized type 316 steel only $M_{23}C_6$ was expected to form after this ageing treatment. The crystal structures and lattice parameters of $M_{23}C_6$ carbides and the intermetallic phase χ observed in this investigation are compared with those reported in the literature in Table III. After cathodic charing, α' and ε martensites were observed.

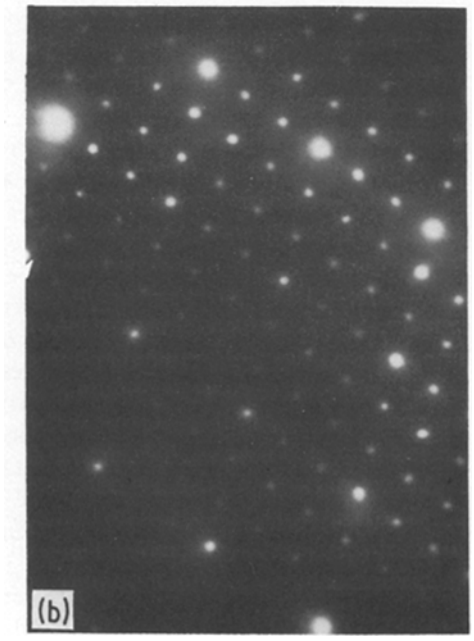

Figure 2 (a) Transmission electron micrograph of carbide precipitation in AISI type 316 sensitized and carburized steel. (b) and (c) SADP taken from $M_{23}C_6/\gamma$ interface and schematic key diagram. ●, $M_{23}C_6$; □, γ.

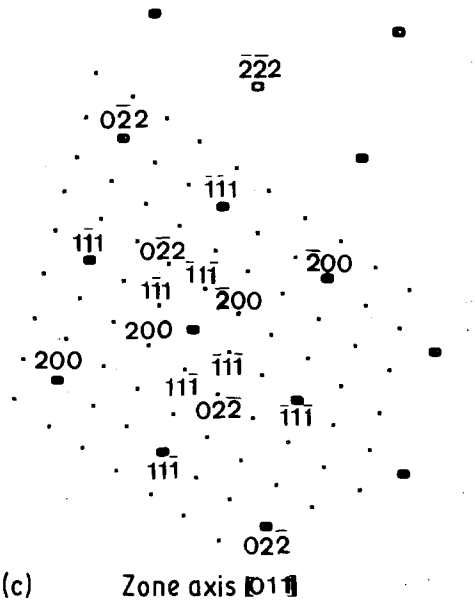

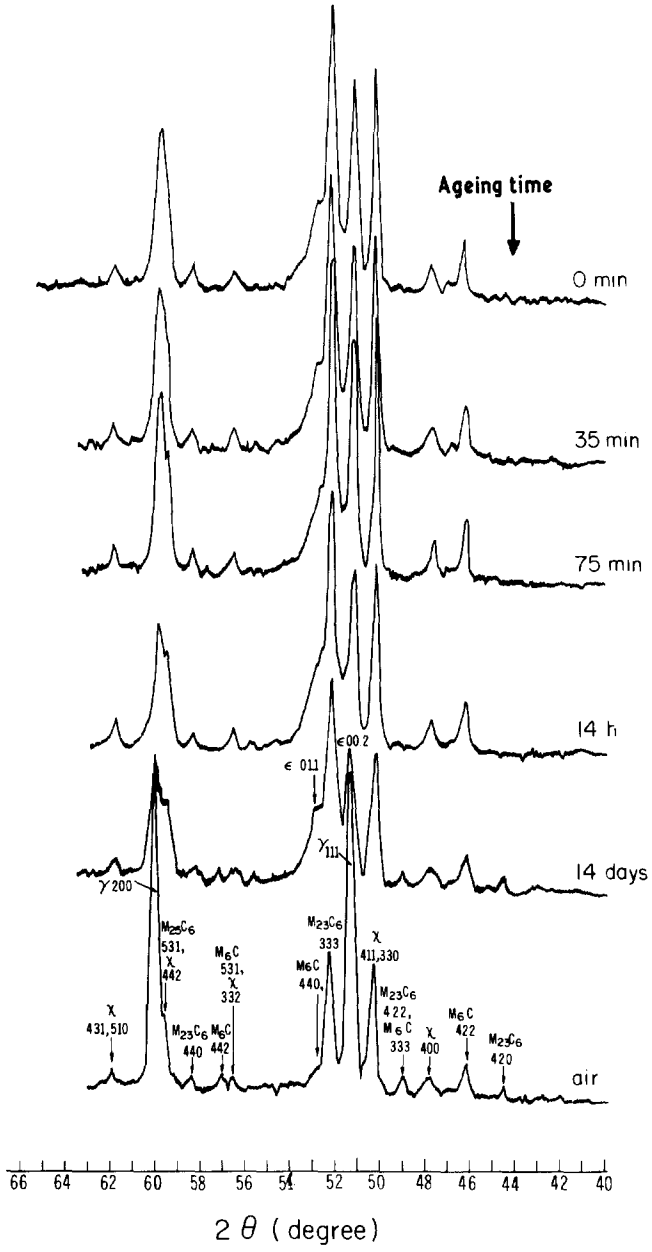

Figure 3 X-ray diffraction patterns of AISI type 316 carburized and sensitized stainless steel, uncharged and originally 24 h cathodically charged after various ageing times at room temperature.

Induced phase transitions by cathodic charging of hydrogen into austenitic stainless steels have also been observed [8–11]. Diffraction peak shifts, line broadening, and the appearance of new reflections were observed after hydrogen charging and during outgassing after charging. Hydrogen penetration considerably expands the lattice of both austenitic and ε-martensitic phases and causes a greater shift in diffraction peaks toward the lower 2θ angles [9]. Hydrogen penetration causes broadening of the γ and ε-phases, which also decreases with time of ageing, when hydrogen is outgassed from the specimen. After ageing the split peaks reformed into two singlets and shifted to the regular position of the uncharged samples. This shift of austenitic peaks is accompanied by a decreasing peak width and after prolonged ageing of 288 h [9], the peak width is approximately the same as for the uncharged sample. However, the peak broadening of ε-martensite decreases with ageing time, but persists even after prolonged ageing of 288 h.

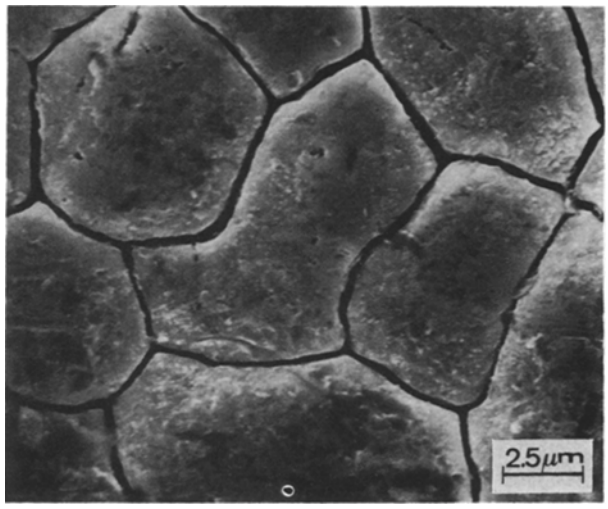

Figure 4 Scanning electron micrograph of surface cracks formed in AISI 316 carburized and sensitized specimens after 24 h cathodic charging.

The nature of the precipitated phases as identified by X-ray diffraction analysis of carburized and sensitized specimens taken after various ageing times is shown in Fig. 3. Diffraction peak shifts to the austenitic γ-phase were observed. The zero shift in the carbides and intermetallic χ-phase peaks, suggests that the phases absorb far less hydrogen than the austenitic matrix.

The stability of the austenite in Fe–Ni–Cr stainless steels is affected by solute hydrogen and stress [9–11]. Evidence of stress relaxation is shown by crack formation in AISI 316 carburized and sensitized specimens after 24 h cathodic charging (Fig. 4). Surface cracking after cathodic charging occurred mainly intergranularly along the grain-boundary carbides in the sensitized samples. The transmission electron micrographs of the sensitized and carburized specimens after cathodic charging are shown (Fig. 5); the plates of hydrogen induced α' martensite. These plates appeared in heavily deformed regions near the grain-boundary carbides. In the sensitized microstructure chromium-depletion occurred to different levels, in certain circumstances [16] down to about 10 wt %. The depleted zones as reported in the literature [16] are of the order of 100 to 300 nm wide, depending on ageing time and temperature.

Hall and Briant [17] studied the chromium distribution in the vicinity of the carbides as a function of sensitization temperature and time in a 316-type austenitic stainless steel using the analytical electron microscope (AEM). Type 304 steel also exhibits intergranular fracture when tested in a sensitized condition, i.e. when chromium depletion occurs at the grain boundaries [18]. Briant [18] suggested that this was caused by a decrease of γ stability and transformation to α' martensite at the grain boundaries. The observation appears to be consistent with decrease in stacking fault energy (SFE) to those observations that demonstrated depletion of chromium near grain boundary carbides [16, 18, 19].

SFE measurements in 309 stainless steel [19] showed that depletion of chromium near boundaries in the

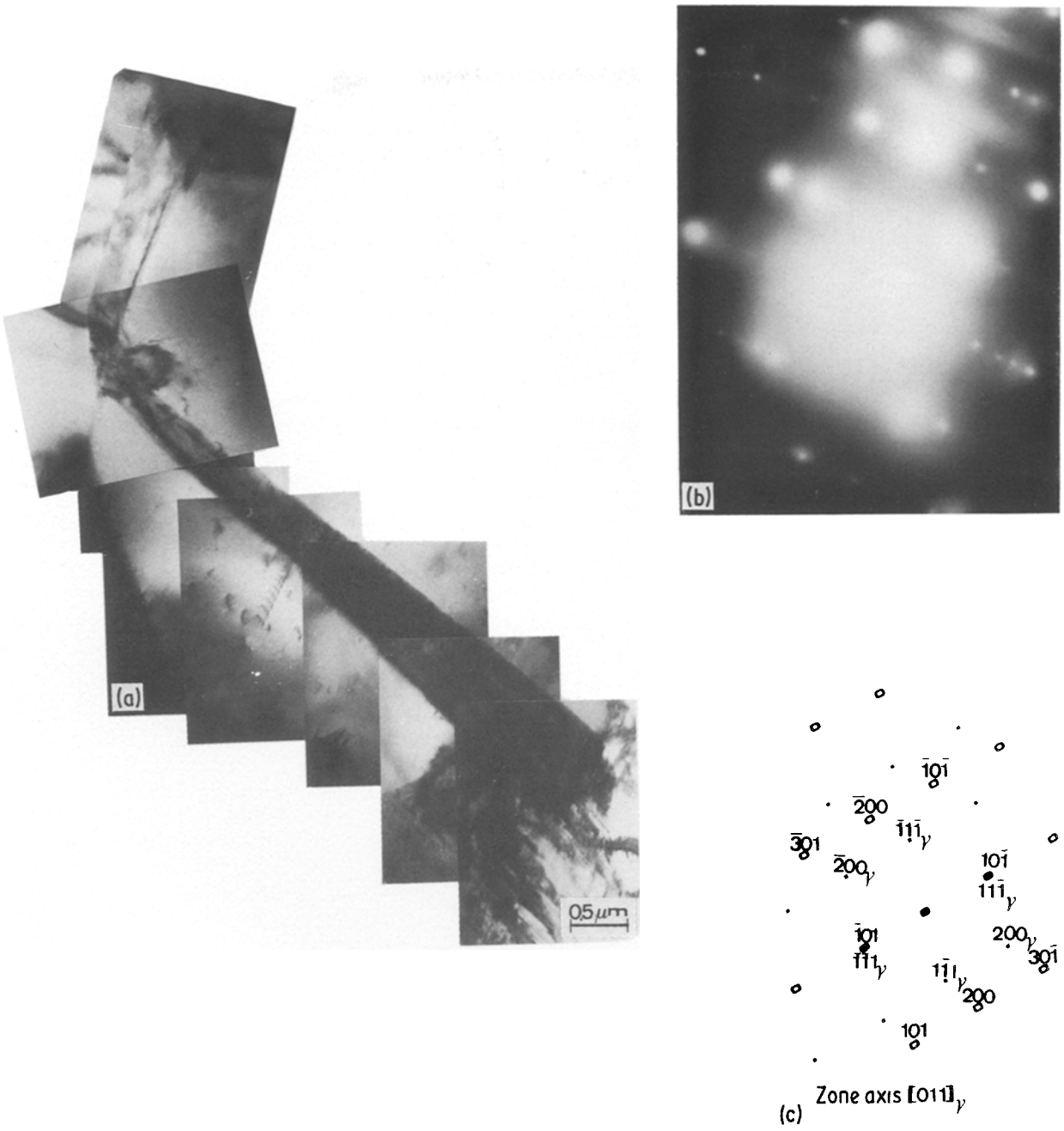

Figure 5 (a) Transmission electron micrograph of α′ martensite near grain boundary carbides in carburized and sensitized steel 24 h hydrogen charged; (b) SADP taken from α′/γ interface, and (c) analysis. ●, γ austenite; □, α′ martensite.

sensitized materials was demonstrated by a stacking fault energy value of about 22 mJ m^{-2}. The matrix value was about 35 mJ m^{-2}. Such a change implies a reduction in chromium from 23% to about 12%, since these regions of additional α′ martensite were only observed after sensitization. The martensite transformation depletion of chromium near grain-boundary areas of significant chromium depletion, where the chemical driving force is a maximum, with pre-existing faults, leads to the development of faulted h c p ε-martensite as an intermediate phase [16]. X-ray diffraction of the same specimens reveals the existence of the ε-martensite (Fig. 3). However, the TEM observations of the high carbon content specimens (2 wt % C) shows only the α′ martensite. If we suppose that the α′ nucleus evolves from the faulted ε, assisted by stress inhomogeneities at the boundary [16], then the dislocation and stacking faults existing close to the carbide interface following precipitation (Fig. 2) indicate additional strain inhomogeneities to the hydrogen charging process.

4. Conclusions

Addition of carbon decreases the time required for sensitization. Short-term (24 h) exposure of this steel to sensitization temperature (650° C) results in a complex precipitation reaction of various carbides ($M_{23}C_6$, M_6C) and intermetallic χ-phase. This study indicates that by X-ray techniques it is possible to detect those precipitates and their behaviour in a hydrogen environment. The zero shifts, as observed by X-ray diffraction, from the carbides ($M_{23}C_6$, M_6C) and the intermetallic χ phase, indicate that these phases absorb considerably less hydrogen than the austenitic matrix. TEM studies reveal that hydrogen induces α′ martensite at chromium-depleted

grain boundaries, near the formation of the carbides.

References

1. C. L. BRIANT, R. A. MULFORD and E. L. HALL, *Corrosion* **9** (1982) 468.
2. B. WEISS and R. STICKLER, *Met. Trans.* **3** (1972) 851.
3. J. K. LAI, *Mater. Sci. Eng.* **58** (1983) 195.
4. *Idem, ibid.* **61** (1983) 101.
5. ASTM Standard E-112 (1977).
6. ASTM Card No. 6-0674 (χ-phase).
7. M. J. DONACHIE Jr and O. H. KRIEGE, *J. Mater. JMLSA* **7** (1972) 269.
8. M. L. HOLZWORTH and M. LOUTHAN Jr, *Corrosion* **24** (1968) 110.
9. P. ROZENAK, L. ZEVIN and D. ELIEZER, *J. Mater. Sci.* **19** (1984) 567.
10. P. ROZENAK and D. ELIEZER, *ibid.* **19** (1984) 3873.
11. N. NARITA, C. J. ALTSTETTER and H. K. BIRNBAUM, *Met. Trans.* 13A (1982) 1355.
12. H. R. KAUTZ and GERLACH, *Arch Eisenhüttenw.* **2** (1968) 151.
13. ASTM Card No. 14-407 ($M_{23}C_6$).
14. ASTM Card No. 11-546 (M_6C).
15. J. S. KASTER, *Acta Metall.* **2** (1954) 456.
16. E. R. BUTLER and M. G. BURKE, in "Proceedings of the International Conference on Martensitic Transformations", edited by L. Delacy and M. Chandrasekaran (Zeuven, Belgium, 1982) p. 121.
17. E. L. HALL and C. L. BRIANT, *Met. Trans.* **15A** (1984) 793.
18. C. L. BRIANT, *ibid.* 10A (1979) 181.
19. A. W. THOMPSON, *Mater. Sci. Eng.* **14** (1974) 253.

Received 13 September
and accepted 12 October 1985